Effect of Soil –Structure Interaction on Seismic Evaluation of Existing Building Frames Resting on Raft Foundation

Dr. Husain Khalaf Jarallah
Department of Civil Engineering
Al-Mustansiriya University
College of Engineering
khalfdce@hotmail.com

***Abstract*- The objective of the present paper is to evaluate the effects of the soil-structure interaction on the seismic evaluation in the building when a framed building is supported on raft foundation. Also the foundation-soil interaction effect has been considered by replacing it with equivalent springs. Nonlinear static pushover analyses of eight-storey reinforced concrete hospital building located at Delhi-India has been performed using the Capacity Spectrum Method of ATC-40. The deformations define the state of damage in the structure through three limit states of the NEHRP Guidelines and the FEMA-356 have been used to evaluate the performance level of the building for drift, the plastic hinge stage of the crack and shear under the condition of the fixed base and the effect of the soil-structure interaction. The performance of the building and individual components has been estimated for Design Basis Earthquake and Maximum Considered Earthquake. The weight of the slab was distributed as triangular and trapezoidal loads to the surrounding beams as per IS 456:2000. The weight of the brick masonry was distributed uniformly on the beams. The results show that the soil structure interaction has marked effect on the roof displacement, storey drift, design base shear, effective damping and crack pattern for beams and columns while there is a minor effect on the torsional behavior of the building. The building is more critical in the performance level when considering the soil flexibility.**

Keywords: Seismic Evaluation; Soil-Structure Interaction; Building, Raft Foundation, Base Shear, Plastic Hinge, Earthquake Engineering, Seismic Analysis, Nonlinear Analysis.

I. Introduction

Frame structures are commonly used in the construction of buildings and industrial structures. The conventional practice considers the isolated behavior of structures during their analysis and design. In reality, however, supporting soil-foundation system alters the behavior of superstructure and hence the need for considering the mutual interaction. It is well known that the response of the structure to earthquake ground-motion will be influenced by deformability of the foundation. Therefore, for a realistic assessment of the response of the structure, this influence should be taken into account. The impact of soil-structure interaction has not been adequately addressed in seismic evaluation of building. In this paper the effect of soil structure interaction (SSI) on seismic evaluation of the eight-storey reinforced concrete existing building resting over raft foundation and located at Delhi-India is presented. The paper discusses the design seismic base shear, roof displacement, storey drift, plastic hinge pattern for beams and columns and torsional behavior of the building.

A nonlinear static pushover analysis of the building has been performed using the Capacity Spectrum Method (CSM) of ATC- 40[1]. For the pushover analysis, the building was modeled in ETABS [2], as a three-dimensional frame with and without soil-structure interaction. Beams and columns were modeled as frame elements with the centre lines joined at nodes. The slabs assumed as a rigid diaphragm. The plastic hinge rotation values corresponding to various Performance Levels have also been taken as per FEMA-356[3], considering the axial force-moment and shear force-moment interactions. The performance point of the building has been estimated using Capacity Spectrum Method. The deformations define the state of damage in the structure through three limit states of the NEHRP Guidelines[4] and the FEMA-356, namely (i) Limit State 'Near Collapse' (NC) level, corresponding to the 'Collapse prevention' (CP) level (ii) Limit State of 'Significant Damage' (SD) level, corresponding to the 'Life Safety' (LS) level and to the single performance level for which new structures are designed according to most current seismic design codes, (iii) Limit State of Damage Limitation (DL) level, corresponding to the 'Immediate Occupancy' (IO) level.

II. The building chosen for the study

The Guru Tegh Bahadur (GTB) Hospital is a large public hospital in the Trans-Yamuna area of Delhi-India has been chosen for this study [5]. Though the site of the hospital has many buildings, this study focused on the eight-storey Ward Block and its connecting corridors and on the physical plant where the major mechanical equipment is located. The original design did not consider the impact of soil structure interaction on building behavior.

The ward blocks are on raft foundation resting on sandy soil of medium stiffness. The foundation has been designed for an allowable bearing capacity of
200kN/m^2 at a depth of 2.5m below original ground level. The thickness of the foundation slab is 1.05m. A 75mm thick lean concrete has been provided under the raft slab. All structural weight and superimposed load on the building is carried by a

system of reinforced concrete slab and concrete beams supported by concrete columns. The storey heights are 3.35m and the slab thickness is 0.13m. The typical framing consists of columns spaced at 3.20 m c/c in the longitudinal direction and (4.13, 2.82 and 7.07) m c/c in the transverse

direction. The clear gap (expansion joint) between two parts is 20 mm. The layout of the ground floor, the orientation of the columns and the view of the 3D modeling are shown in Fig. (1).

Lateral forces in each direction are resisted by perimeter spandrel beam-column frames as well as interior beam-column frames. The beam (400mmx500mm) and column (400mmx600mm) sizes are same at all the floors (Fig.(1)). There are similarities in the reinforcement of the columns for two successive storeys. The re-bars of columns are having sufficient development length into the raft. The columns are cast at site monolithic with the raft. Table (1) presents the material properties obtained from available drawings [5]. The specified values can significantly underestimate the actual strength (referred to hereafter as the "expected" strength) of the in-situ material. The "expected" values are always larger than the "specified" values because of the inherent overstrengths in the original material and strength gained over time. Furthermore, concrete exhibits a significant increase in both strength and stiffness and reinforcing steel in strength when subjected to increased strain rates, e.g. at strain rates that are expected during earthquake.

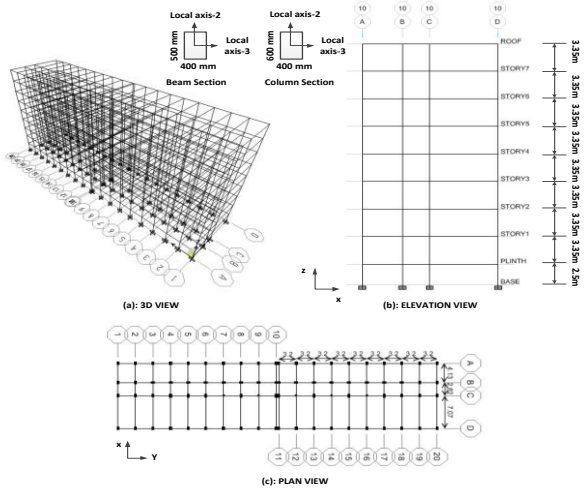

Fig. 1 3D Computer model and geometry of the building.

Table I Properties of construction materials

Concrete			Steel	
Member	Column	Beam	Yield strength (MPa)	415
Grade	M25	M15		
Specified characteristics compressive strength of 150 mm cube at 28 Days (MPa)	25	15	Expected yield strength (MPa)	497
Specified Cylinder strength (MPa)	20	12		
Expected cylinder strength (MPa)	25.6	16.8		

III. Properties of soils

The bearing stiffness of a vertically loaded plate on soil materials is a function of the dimensions of the plate, the depth of bearing plane beneath the surface, and the properties of the soil materials. The shear modulus, G, for a soil is related to modulus of elasticity, E, Poisson's ratio, ν, and Shear wave velocity, v_s, and Mass density of soil, ρ, by the relationship[3],

$$G = \rho v_s^2 \quad \ldots\ldots (1)$$

$$E = 2G(1+\nu) \quad \ldots\ldots (2)$$

IV. Modeling of soil-foundation

The following three different methods, are commonly used for analyzing soil structure interaction (SSI) problem i.e., frame–foundation-soil system, under static loads;

1. The spring analogy method
2. Iterative method and
3. Finite element method.

The spring analogy method has been used in this study for the simplicity and the because of the main objective of the study is the evaluation of seismic performance for the super-structure of the building.

Within the ambit of linear elasticity, in the present study Winkler springs model was used. In Winkler's model, the soil mass is represented by a series of linear independent springs (Fig.(2) [3]). Hence the shear resistance of soil is not taken into account and the reaction force acting on foundation at any point is directly proportional to the foundation settlement at that point. The pressure settlement relation is given as;

$$P_i = K_s W_i \quad \ldots\ldots (3)$$

where,

P_i = pressure at any point i.

W_i = settlement at the point i.

K_s = coefficient of sub grade reaction of the soil or unit sub grade modulus.

In addition, stiffness coefficient K_{ii}, which is defined as load per unit deformation, is given by;

$$K_{ii} = K_s\, Ab \quad \ldots\ldots (4)$$

where 'Ab' is the area over which P_i is acting.

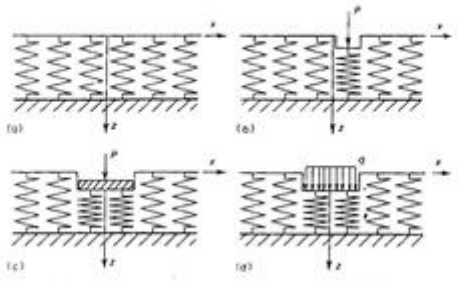

Fig. 2 Deformations of Winkler Model, Shown Unloaded in (a), Due to a Concentrated Force (b), Rigid Load (c) and Uniform Flexible Load (d) [3].

V. Calculation of stiffness' of elastic springs elements for raft foundation

The flexibility of soil is usually modeled by inserting the discrete spring elements between the foundation members and the soil medium (Winkler springs model). The spring constants are determined from elastic half space solution. The following expressions given by Pais and Kausel [7] have been used in present study for account the flexible behavior of soil below the rectangular raft footing;

Vertical:

$$K_V = K_V^o \left[1.0 + \left(0.25 + \frac{0.25}{L/B}\right) (D/B)^{0.8}\right] \quad \text{.....(5)}$$

Horizontal:

$$K_H = K_H^o \left[1.0 + \left(0.33 + \frac{1.34}{1+L/B}\right) (D/B)^{0.8}\right] \quad \text{.....(6)}$$

where:

$$K_V^o = \frac{G\,B}{(1-\nu)} \left(3.1\left(\frac{L}{B}\right) + 1.6\right) \quad \text{.....(7)}$$

$$K_{H_Y}^o = \frac{G\,B}{(2-\nu)} \left(6.8\left(\frac{L}{B}\right)^{0.65} + 2.4\right) \quad \text{.....(8)}$$

$$K_{H_X}^o = \frac{G\,B}{(2-\nu)} \left(K_{H_y}^o \frac{(2-\nu)}{G\,B} + 0.8\left(\frac{L}{B} - 1\right)\right) \quad \text{.....(9)}$$

and; ν is the Poisson ratio, G shear modulus and 2L, 2B and D are dimension of footing as shown in Fig. (3). The stiffness values so obtained at the Center of Gravity (C.G.) of the raft foundation are distributed all the springs as series or parallel connections according to the respective directions as shown in Fig.(4). The values of the vertical and horizontals stiffness derived from above equations in X, Y and Z directions respectively are given in Fig. (3) below.

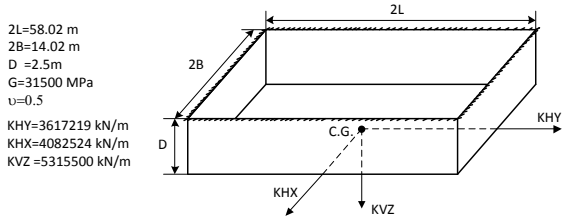

Fig. 3 Rectangular embedded foundation (L ≥ B).

VI. Mathematical modeling of building frames

Each individual block is separated by expansion joints of 20 mm in more or less symmetric manner. The building was modeled as a three-dimensional frame with a fixed base and with spring to calculate the response of the structure. In the transverse direction, there are four beam-column frames while in the longitudinal direction, there are 20 such frames (10 frames for each part). All elements are believed to contribute to the lateral resistance of the building. Beams and columns were modeled as frame elements with the centrelines joined at nodes, with 6 degrees of freedom at each joint. The building has two parts A and B. These are taken as connected by rigid links. The rigid beam-column joints were neglected by giving rigid zone factor equal to zero in the modeling. Fig (1) shows the three-dimensional computer model of the building. The weight of the slab was distributed as triangular and trapezoidal loads to the surrounding beams.

VII. Raft foundation modeling

The structural raft model and the geotechnical soil model interact by means of the soil spring. These supported the raft and transmit the reactions from the raft to the soil model. In the present study, the raft has been modeled as a slab of two-dimensional four-noded plate finite elements. The support offered by the foundation soil is modeled by discrete 'soil spring'. The springs were positioned under each column, and at a uniform grid spacing between columns equivalent to about 20% of the distance between adjacent columns [8], as shown in Fig.(4). The soil springs were positioned only at the corners of the plate element. The total number of node assign with the soil spring for raft foundation is equal to 1472. The soil spring values for typical node are shown in Fig. (4).

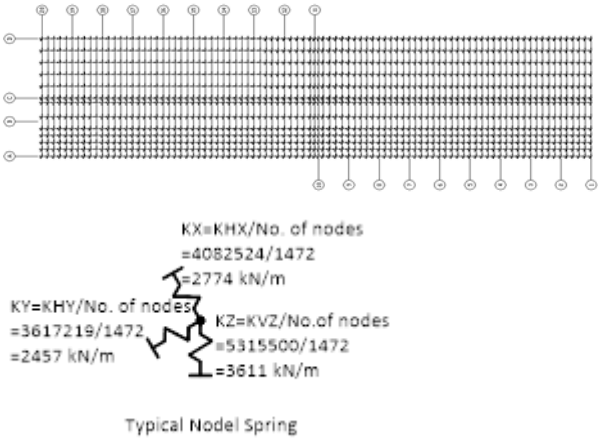

Fig. 4 Finite element modeling of raft foundation and soil spring.

VIII. Nonlinear modelling of reinforced concrete frames

A three-dimensional model of each structure is created in ETABS to carry out nonlinear static analysis. Beam and column elements are modeled as nonlinear frame elements with lumped plasticity by defining plastic hinges at both ends of the beams and columns.

Plastic hinge properties can be characterized by a typical elastic-plastic force-deformation relationship with strength degradation at high ductility demands as shown in Fig. (5). Compliant behavior generally, as shown in Fig. (5), will be modeled using nonlinear load-deformation relations defined by a series of straight-line segments (FEMA-356). In this Fig, Q_{CE} refers to the strength of the component and Q refers to the demand imposed by the earthquake. As shown in Fig, the response is linear up to an effective yield point, B, followed by yielding (possibly with strain hardening) to point C, followed by strength degradation to point D, followed by final collapse and loss of gravity load capacity at point E.

The following main points relate to the depicted load deformation

- Point A corresponds to the unloaded condition. The analysis must recognize that gravity loads may induce initial forces and deformations that should be accounted for in the model.
- Point B has resistance equal to the nominal yield strength. Usually, this value is less than the nominal strength.
- Slope between points B and C is taken as 10% total strain hardening for steel.

- The abscissa at C corresponds to the deformation at which significant strength degradation begins. Beyond this deformation, continued resistance to reversed cyclic lateral forces can no longer be guaranteed. For brittle components, this deformation is the same as the deformation at which yield strength is reached.
- The drop in resistance from C to D represents initial failure of the component.
- Point E is a point defining the maximum deformation capacity.
- Points C, D and E are based on FEMA-356.
- My is based on reinforcement provided.

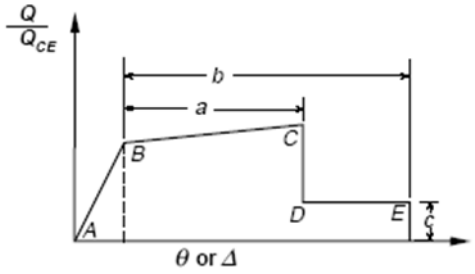

Fig. 5 Idealized component load versus deformation curves for depicting component modeling and acceptability.

Since deformation ductility is not a primary concern, the point B is not the focus, and it is obtained from ETABS using approximate component initial effective stiffness values according to ATC-40 (Table (2)) for beams and columns, respectively.

Table II Component initial stiffness

Component	Flexural rigidity	Shear rigidity	Axial rigidity
Beam	0.5 Ec Ig	0.4 Ec Aw	Ec Ag
Column	0.7 Ec Ig	0.4 Ec Aw	Ec Ag

where, Ec is modulus of elasticity of concrete, Ig is moment of inertia of gross concrete section about centroidal axis, neglecting reinforcement, Aw is area of concrete section resisting shear transfer and Ag is gross area of concrete section.

8.1 Concrete Column Modeling

Fig (6) illustrates axial force-moment interaction diagram for a typical A1 and D1 perimeter frame column between 3rd and 4th floors (A1 and D1 refers for columns located at grids A-1 and D-1 respectively (Fig. (1))). Similar analyses were performed for the columns at the other floor levels. As noted earlier, "expected" values were used for the steel and concrete strength to calculate all capacities. The columns between 3rd and 4th floors (A1 and D1 frames) typically consist of 16-ϕ16.

8.2 Beam Modeling

Fig (7) illustrates the moment curvature diagram of typical 3rd and 4th (B6-B7) floor beams in the longitudinal direction. Typical stirrups consist of ϕ8 ties at 75 mm and 125 mm c/c near the two ends and 250 mm c/c in the middle portion. For reinforcement, this beam has 2- ϕ20, 3- ϕ25 at the top and 5- ϕ20 at the bottom.

IX. Nonlinear plastic hinge properties

The building has to be modeled to carry out nonlinear static pushover analysis. This requires the development of force-deformation curve for the critical sections of beams, columns by using the guidelines of FEMA 356 as mentioned above. The force-deformation curves in flexure were obtained from the reinforcement details given in the drawings [5] and were assigned for all the columns and beams. The nonlinear properties of beams and columns have been evaluated using the software section designer for ETABS and have been assigned to the computer model in ETABS. The flexural hinges (M3) were assigned for the beams at two ends. The interacting P-M2-M3 frame hinge type, a coupled hinge property, was also assigned for all the columns at upper and lower ends. The points A, B, C, D and E are marked on the curve shown in Fig. (8 B is the point at which the section yields; at point C, unloading occurs upto point D, which is the point at which the section reaches its residual capacity and then it starts deforming upto point E with a residual capacity. The other salient points are Immediate Occupancy (IO), Life Safety (LS) and Collapse Prevention (CP) equally spaced in the region BC. Hinge properties required in ETABS need to be defined only for plastic portion. The elastic behavior of the frame element is determined by the frame section (and hence material properties) assigned to the element. Thus, the linear behavior of the structure is not changed by the assignment of hinges to the frame elements. The coordinate values of the B,C , D and E have been used as (0,1.0), (0.003,1.1), (0.003,0.2), (0.01,0.2) for column and (0,1.0), (0.02,1.1), (0.02,0.2), (0.03,0.2) for beams, as per ATC-40 and FEMA 356. Further the values of IO, LS and CP have been used as 0.005, 0.01, 0.02 and 0.002, 0.0015, 0.003 for columns and beams respectively.

The force-deformation curve in shear was obtained from the reinforcement details given in the drawing and was assigned in all the columns and beams. The shear hinges (V2) were assigned for the beams at two ends. Shear hinges (V2 and V3) were given for all the columns at mid height taking into account the orientation for the columns. A typical force-deformation curve is given in Fig. (8). The development of shear force-deformation curve for the critical sections of beams, columns has been obtained by using the guide lines of FEMA-356. FEMA-356 does not define the values of plastic deformation for shear in Primary Columns. Therefore the shear action in columns has been modeled as Force Controlled, by giving very low values (1/100 of those for beams) for plastic deformation corresponding to IO, LS, CP, etc. For beam the contribution of concrete shear strength is calculated according to ACI-318[9]. For column, the contribution of concrete shear strength, calculated according to FEMA-356. For beam and column, the contribution of steel shear strength is calculated according to ATC-40.

X. Lateral load distributions

The pushover analysis determines the levels of building lateral forces and corresponding roof displacements that are associated with successive stages of the development of yielding in the building members. Lateral forces are applied in proportion to the storey masses and the square height of the floor as per IS 1893:2002[10]:

$$F_i = \frac{m_i \, h_i^2}{\sum_{j=1}^{n} m_j \, h_j^2} \quad \text{.....(10)}$$

where, m_i and h_i are the mass and height of i^{th} or j^{th} floor from the base, n is number of storeys .

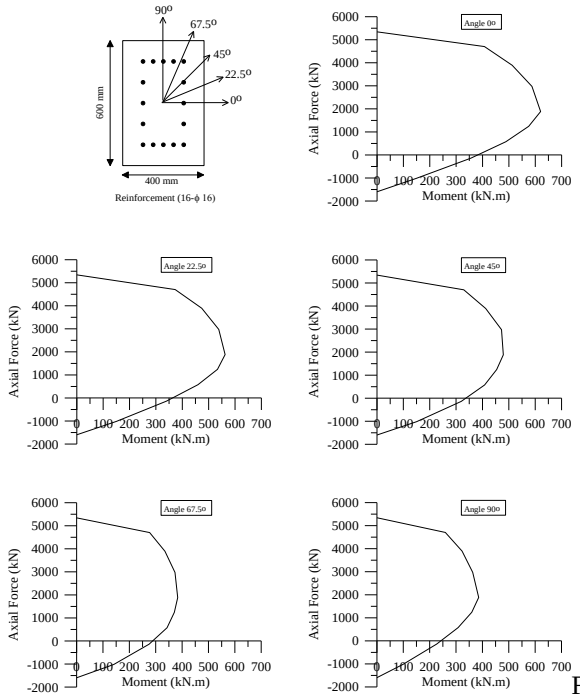

Fig. (6 Existing column interaction diagram at 3rd and 4th floors.

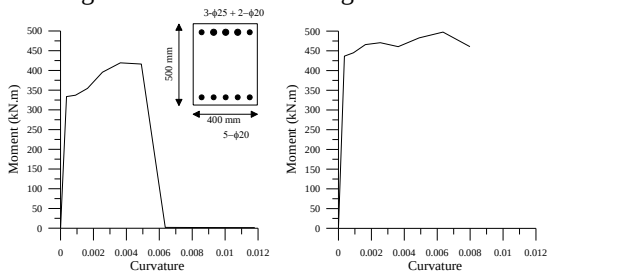

(a)Positive Moment (Yield Moment = 333.7 kN.m) (b)Negative Moment (Yield Moment = 436.50 kN.m)

Fig. 7 Existing beam moment-curvature diagram at 3rd and 4th floors.

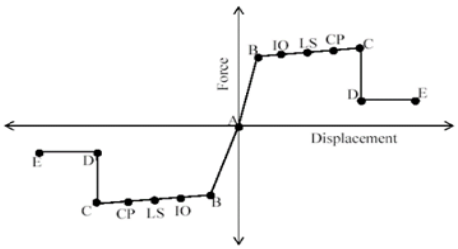

Fig. 8 Force-deformation curve for beams and columns

The initial load distribution was used throughout the analyses for each respective direction. The same distribution of lateral load is taken for pushover analyses in both X and Y directions (Fig. (9)).

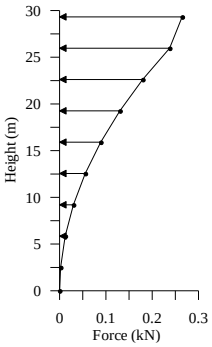

Fig. (9 Lateral load distribution along height.

XI. Design base shear as per is1893:2002 code

Design base shear as per IS 1893:2002 is define by

$$V_b = A_h \, W \quad \text{.....(11)}$$

where W= seismic weight and A_h is the design horizontal seismic coefficient for a structure which is determined by the following expression:

$$A_h = \frac{z \; I \; S_a}{2 \; R \; g} \quad \text{.....(12)}$$

where *z*= zone factor for the Maximum Considered Earthquake (MCE) in a particular zone. The factor 2 in the denominator of z is used so as to reduce the Maximum Considered Earthquake (MCE) to Design Basis Earthquake (DBE). I= importance factor, depending upon the functional use of the structures, characterized by hazardous consequences of its failure, post-earthquake functional needs, historical value, or economic importance. R = response reduction factor, depends on the perceived seismic damage performance of the structure, characterized by ductile or brittle deformations. However, the ratio (I/R) shall not be greater than 1.0. S_a/g =average response acceleration coefficient for rock or soil sites as given in IS: 1893:2002. The seismicity was defined by the elastic spectrum defined in IS: 1893:2002 for 5% damping (Fig. (10)).The building is located in zone IV, i.e., seismic zone factor z=0.24. The building is considered to be ordinary reinforced concrete moment-resisting framed building (OMRF) (R=3).The seismic weight (W=102662 kN).The importance factor (I) is taken as 1.5. Table (3) shows the design base shear calculated from the code formula and for time period obtained from modeling with different reduction factors. The design base shear for fixed greater than for SSI.

Table III Design base shear

Direction	Design base shear (kN)			
	Fixed base		SSI	
	R=5	R=3	R=5	R=3
X	2762	4603	2234	3723
Y	2604	4340	2539	4232

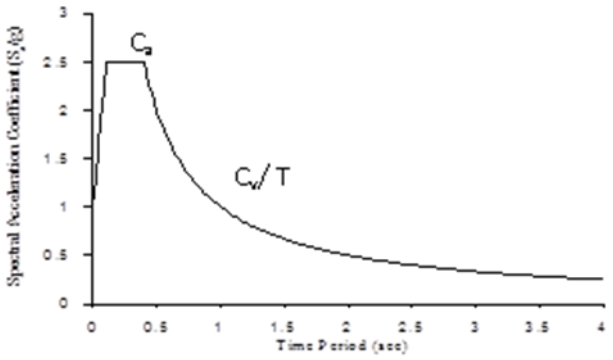

Fig. (10 Response spectrum for 5% damping according IS: 1893-2002.

XII. PUSHOVER ANALYSIS

The pushover analysis consists of the application of gravity loads and a representative lateral load pattern. The frames were subjected to gravity analyses and simultaneous lateral loading. Gravity loads were in place during lateral loading. In all cases, lateral forces were applied monotonically in a step-by-step nonlinear static analysis. The applied lateral forces were triangular shape as per IS 1893:2002 and given in equation (11) above. P–Delta effects were taken into account. In pushover analysis, the behavior of the structure is characterized by a capacity curve that represents the relationship between the base shear force and the displacement of the roof. This is a very convenient representation in practice, and can be visualized easily by the engineer. It is recognized that roof displacement was used for the capacity curve because it is widely accepted in practice. The floor and roof slabs have been considered as rigid diaphragm. The building has been first analyzed under the action of the dead load acting on the structure. The forces in the members due to dead loads are taken as the initial forces in the structural members for studying the inelastic behavior of the building subjected to the lateral forces. The weight of the slab was distributed as triangular and a trapezoidal load to the surrounding beams as per IS 456:2000[11]. The weight of the brick masonry was distributed uniformly on the beams. To consider the uncertainties in the dead load estimation, it was multiplied by a factor of 1.1. Live load has been considered in combination with earthquake load. It is assumed that the live load present at the time of earthquake will be taken care of by the 10% increase in the dead load. The gravity loads were assigned to all the beams and analysis is done for the gravity loads (1.1 DL) under load control. The lateral pushover analysis (in X and Y direction) was followed after the gravity pushover, under displacement control. The building is pushed in lateral directions until the formation of collapse mechanism (ATC-40). The capacity curve (Base shear versus Roof displacement) is obtained in X and Y directions.

XIII. Results and discussion

13.1 Capacity Curves

The capacity curves (Base shear vs. roof displacement capacities) are generated for the building with and without soil structure interaction in X and Y directions as shown in Fig. (11). In both cases, lateral forces are applied monotonically with step-by-step nonlinear static analysis (displacement controlled) over the stresses found on structure from gravity load analysis. From the nonlinear static analysis, it is observed a remarkable difference in base shear capacities of models with and without soil-structure interaction. The base shear in case 4 has a high capacity of 660 kN, whereas for case 1, the base shear is found to be 360 kN.

13.2 Capacity Spectrum Analysis

The capacity curves obtained are converted to corresponding capacity spectra using Acceleration - Displacement Response Spectra (ADRS) format (recommended in ATC-40) and overlapped with code conforming Design Basis Earthquake (DBE) and Maximum Considered Earthquake (MCE) demand spectra of IS: 1893–2002 as shown in Figs (12) and (13). The zone factor (z) for Delhi is taken as 0.24. The demand spectrum for DBE is obtained from peak ground acceleration (PGA) of (z/2×g = 0.12g). The soil condition has been considered as medium and Cv has been taken as 1.36z/2 for medium soil as per IS: 1893. The demand spectrum is plotted with Ca = 0.12g, Cv = 1.36×0.12g = 0.1632g, and 5% initial damping. Status of performance points is given in Table (9). The demand spectrum is plotted with Ca = 0.24g, Cv = 1.36×0.24g, and 5% initial damping. Status of performance point is given in Table (4). The performance points observed on DBE and MCE with importance factor (I) = 1.5 are shown in Table (4).

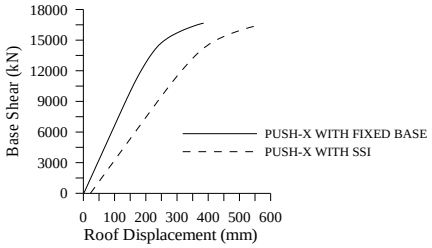

Base Shear and Roof Displacement in X-direction for original Building

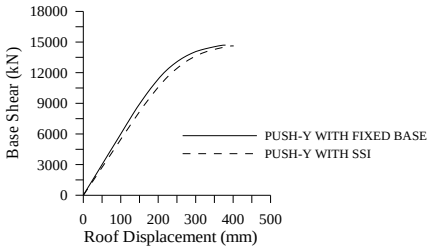

Base Shear and Roof Displacement in Y-direction for original Building

Fig. 11 Base shear vs roof displacement.

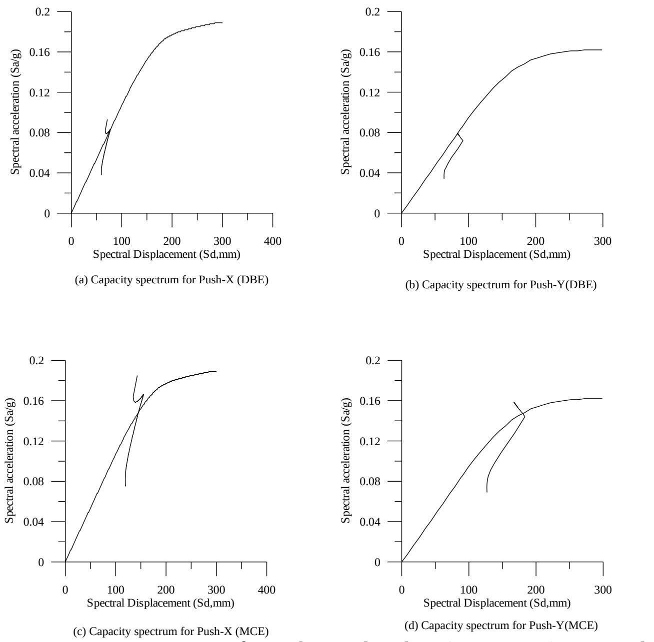

Fig. 12 Capacity spectrum for Push-X and Push-Y (DBE, MCE) For Fixed base.

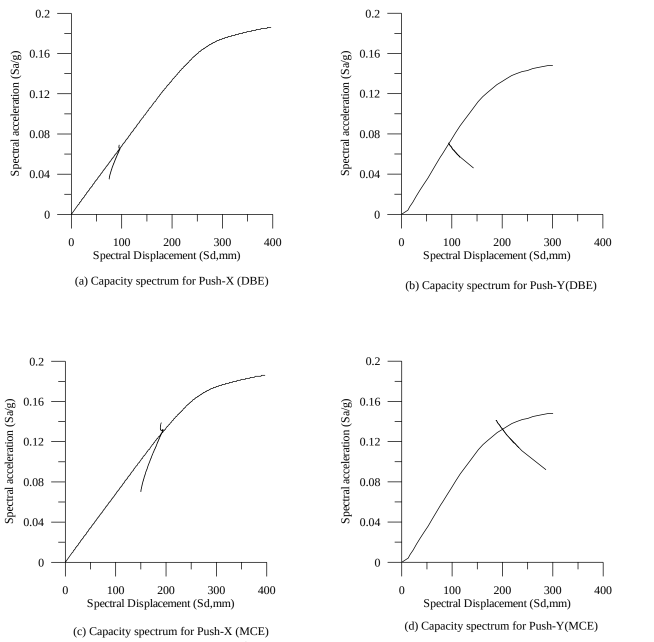

Fig. 13 Capacity spectrum for Push-X and Push-Y (DBE, MCE) with SSI.

XIV. Safety of existing structures

14.1. Safety for Drift

The safety for the building has been checked from the drift ratio and compares with the deformation limits as given in ATC-40.The maximum drift ratios are given in Table (5) for CSM. Fig (14) shows the storey drifts at center of mass of each floor corresponding to performance points under DBE and MCE in X and Y directions. The storey drifts are compared with the roof drift ratios in the two directions under DBE and MCE.

The safety of the existing structures has been checked under dead load as well as under earthquake loads. It has been found that the building is safe against earthquake loading. The displacements at roof and base shear at performance level are shown in the Table (5) for DBE and MCE.

14.2. Safety for Crack

The plastic hinges of longitudinal frames A, B, C and D in X and Y-directions at the target displacement are shown in the Figs (15) and (16). The status of the performance point in terms of the number of hinges is given in Table (6).

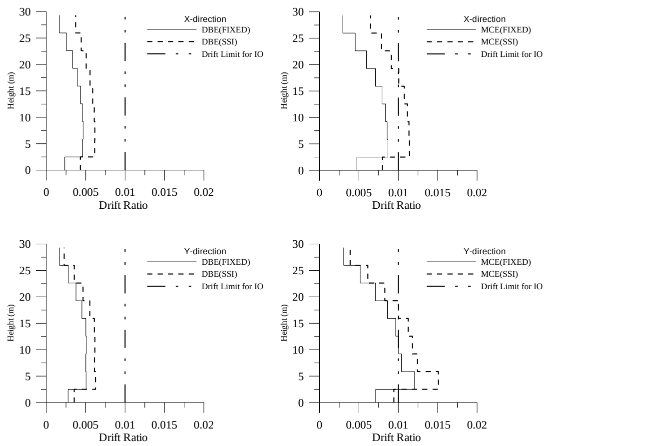

Fig. 14 Storey drift ratio for DBE and MCE in X and Y directions for both cases.

XV. Torsional behavior

The lateral displacement is slightly different at the two ends of the building in X direction. The maximum ratios of maximum horizontal displacement to average horizontal displacement are 1.01, 1.014, 1.004 and 1.02 in X and Y direction respectively. Figs (17) and (18) shows the storey displacement of the individual frames (refer Fig. (1) for Frame 1, Frame 11, Frame 20,Frame A and Frame D) as obtained from the pushover analysis along X-direction and Y-direction for building with and without soil-structure interaction. The Fig shows the results of pushover analysis in the X and Y directions for DBE and MCE for both cases. As shown in the Fig there is no torsion in the building.

XVI. Check for shear

For beam the contribution of concrete shear strength, V_c, calculated according to Eqn.(10) as per ACI-318;

$$V_c = 0.17\sqrt{f'_c}\, b\, d \;\ldots\ldots\ldots\ldots\ldots\ldots\ldots\ldots\ldots\ldots\ldots\ldots\ldots\ldots\ldots\ldots\ldots\ldots\ldots\ldots.. (13)$$

For column, the contribution of concrete shear strength, V_c, calculated according to equation (11) as per FEMA-356,

$$V_c = \lambda\, k \left(\frac{6\sqrt{f'_c}}{M/Vd} \sqrt{1 + \frac{N_u}{6\sqrt{f'_c}\, A_g}} \right) \left(0.8\, b_w\, h\right) \ldots (14)$$

In which k=1.0 in regions of low ductility demand, 0.7 in regions of high ductility demand, and various linearly between theses extremes in regions of moderate ductility demand ;λ=0.75 for lightweight aggregate concrete and 1.0 for normal weight aggregate concrete; N_u=axial compression force in pounds(=0.0 for tension force); M/V is the largest ratio of moment to shear under design loadings for column but shall not be taken greater than 3 or less than 2 ; d is the effective depth ; and A_g is the gross-sectional area of column. k=1.0 and λ=1.0 for this building.

For beam and column the contribution of steel shear strength, V_s, calculated according to Eqn.(12)

$$V_S = \frac{A_V f_y d}{S} \quad \text{.....(15)}$$

The columns have four legged and six legged stirrups at a spacing of 250 mm c/c throughout their length. All the columns and beams are found safe in shear for the case of with and without soil structure interaction effect.

XVII. CONCLUSIONS

Based on the investigations carried out in this study on the influence of soil flexibility on the on seismic performance evaluation of existing reinforced concrete buildings resting on raft footing the following conclusions are drawn:

I. Modeling of soil using soil spring in the three orthogonal directions provide a viable means for carrying out studies the on seismic performance evaluation of existing reinforced concrete buildings resting on raft footing.

II. If the flexibility of the soil is not considered, the seismic performance evaluation of reinforced concrete building will be underestimating.

III. A significant variation is observed in base shear capacities and hinge formation mechanisms for two cases with and without soil flexibility at yield and ultimate.

IV. Based on the observations in the hinging patterns, it is apparent that the plastic hinge number where details of hinges falling in collapse prevention and ultimate strength range more in the case of the seismic performance evaluation considering soil flexibility compared with the case of fixed base.

V. The safety for the building has been checked from the drift ratio and compare with the deformation limits as given in ATC-40.The maximum drift ratios and corresponding Performance Level are more critical in the case of the seismic performance evaluation considering soil flexibility compared with the case of fixed base.

VI. There is slightly impact of soil-structure interaction on the torsional behavior of the building.

VII. The beams and columns have been checked and found safe for the expected shear force at performance point.

XVIII. References

[1] Applied Technology Council, 1996, "Seismic Evaluation and Retrofit of Concrete Buildings", Report No. SSC 96-01: ATC-40, Vol.1, Redwood City, California, 14-7 p.

[2] ETABS plus Version 9.7.1, "Extended 3-D Analysis of Building Systems", Computer and Structures, Inc., Berkeley, CA, USA.

[3] Federal Emergency Management Agency, 2000, "Prestandard and Commentary for the Seismic Rehabilitation of Buildings", FEMA-356, Washington, D.C, 11-44 p.

[4] Federal Emergency Management Agency, 1997, "NEHRP Guidelines for the Seismic Rehabilitation of Buildings", FEMA-273, Washington, D.C, 11-31 p.

[5] Jarallah, H.K., Singh,Y. and Paul,D. K., (2006), "Nonlinear Static (Pushover) Analysis of GTB Hospital (Ward Block)", Technical Report No. EQ: 2006-10, Department of Earthquake Engineering, Indian Institute of Technology Roorkee, India, 69 p.

[6] Choudhary, K.U., 2003, "Study Of Soil-Structure Interaction in 2D/3D Building Frames", M.Tech. Thesis, Department of Civil Engineering, Indian Institute of Technology Roorkee, India, 71 p.

[7] Pais, A. and Kausel, E., 1988, "Approximate Formulas for Dynamic Stiffnesses of Rigid Foundations", Soil Dynamics and Earthquake Engineering, Vol.7, No.4, pp. 213-227.

[8] Hemsley, J.A., 2000, "Design Application of Raft Foundation", Published by Thomas Telford Ltd. London, 626 p.

[9] ACI committee 318, 2008," Building Code Requirements for Structural Concrete (ACI 318M-08) and Commentary", American Concrete Institute, Michigan, 473 p.

[10] Indian Standard Criteria for Earthquake Resistant Design of Structures, IS 1893: (Part 1) 2002, Part 1 General Provisions and Buildings (Fifth Revision), Bureau of Indian Standards, New Delhi, India, 39 p.

[11] Indian Standard Code of Practice for Plain and Reinforced Concrete (Fourth Revision), IS 456: 2000, Bureau of Indian Standards, New Delhi, India, 100 p.

XVIII. Notation and abbreviations

Ab	Area over which P_i is acting
ADRS	Acceleration-Displacement Response Spectra
A_g	Gross area of concrete section
A_h	Design horizontal seismic coefficient
Av	Area of shear reinforcement within spacing S
A_W	Area of concrete section resisting shear transfer
b_w	Width of the reinforced concrete member cross-section.
Ca	The seismic coefficient represents the effective peak acceleration (EPA) of the ground.
CP	Collapse prevention
CSM	Capacity Spectrum Method
Cv	The seismic coefficient represents 5 percent-damped response of a l-second system and when divided by period defines acceleration response in the velocity domain.
d	The effective depth
D,2B, 2L	Dimensions of the foundation: Length, width, depth
DBE	Design basis earthquake
DL	Damage limitation
E	Modulus of elasticity
E_C	Modulus of elasticity of concrete
Fi	Lateral forces at the floor i
f'_c	Specified compressive strength of concrete
fy	Specified yield strength of reinforcement
G	Shear modulus
g	Acceleration due to gravity
hi	The height of ith floor

I	Importance factor
Ig	Moment of inertia of gross concrete section about centroidal axis, neglecting reinforcement
IO	Immediate occupancy
KHX, KHY, KVZ	Static stiffness for a rigid plate on semi-infinite homogeneous elastic half-space.
$K^o_{HX}, K^o_{HY}, K^o_V$	Surface stiffness for a rigid plate on semi-infinite homogeneous elastic half-space.
K_{ii}	Stiffness coefficient
Ks	Coefficient of sub grade reaction of the soil or unit sub grade modulus
KX,KY, KZ	Elastic stiffness of the equivalent spring
LS	Life safety
M	Moment under design loadings
M2, M3	The moments about local 2 and 3-axes
MCE	Maximum considered earthquake
mi	Mass of i^{th} floor
n	Number of storeys
NC	Near Collapse
Nu	Axial compression force
OMRF	Ordinary reinforced concrete moment-resisting framed building
P	Axial load
PGA	Peak ground acceleration
Pi	Pressure at any point i
q	Uniform flexible load
Q	Demand imposed by the earthquake
Q_{CE}	Strength of the component
R	Response reduction factor
S	Center-to-center spacing of items, such as longitudinal reinforcement, transverse reinforcement
Sa	Spectral acceleration
Sa/g	Average response acceleration coefficient for rock or soil sites as given in IS: 1893:2002
SD	Significant Damage
SSI	Soil-structure interaction
T	Fundamental period of the structure
V	Shear under design loadings
V2,V3	Shear force in 2 and 3 direction
Vb	Seismic base shear
V_c	Nominal shear strength provided by concrete
v_s	Shear wave velocity
Vs	Nominal shear strength provided by shear reinforcement
W	Seismic weight of the structure
Wi	Settlement at the point i
X,Y,Z	Global axis
z	Zone factor
ρ	Mass density of soil
λ	Modification factor reflecting the reduced mechanical properties of lightweight concrete
ν	Poisson's ratio

Table IV Status of performance points

Condition	Direction	Earthquake level	Vb (kN)	Spectral Acceleration Sa/g	Effective Time Period Teff (sec)	Roof Displacement Δ_{roof} (mm)	Spectral Displacement Sd (mm)	Effective Damping β_{eff}
Fixed base	X	DBE	6905	0.083	1.939	104	78	0.053
		MCE	12410	0.148	1.985	193	145	0.074
	Y	DBE	6662	0.079	2.063	111	84	0.05
		MCE	12664	0.147	2.216	236	180	0.05
SSI	X	DBE	5573	0.066	2.431	156	97	0.054
		MCE	10887	0.128	2.45	285	191	0.058
	Y	DBE	7687	0.07	2.318	141	94	0.05
		MCE	13240	0.132	2.465	281	200	0.05

Table V Roof Displacement, Base Shear Forces and drift at Performance Level

Condition	Direction	Earthquake level	Disp.(mm)	Base Shear(kN)	Maximum Drift Ratio	Performance Level
Fixed base	X	DBE	106	7007	0.0047	Immediate Occupancy
		MCE	193	12458	0.0087	Immediate Occupancy
	Y	DBE	117	7042	0.0051	Immediate Occupancy
		MCE	240	12787	0.0121	Damage Control
SSI	X	DBE	156	5596	0.0062	Immediate Occupancy
		MCE	285	10889	0.0114	Damage Control
	Y	DBE	147	8034	0.0062	Immediate Occupancy
		MCE	292	13476	0.0151	Damage Control

Table VI Number of hinges in each range at performance point

Condition	Direction	Earthquake level	A-B	B-IO	IO-LS	LS-CP	CP-C	C-D	D-E	>E	TOTAL
FIXED	X	DBE	3723	1	0	0	0	0	0	0	3724
		MCE	3510	212	2	0	0	0	0	0	3724
	Y	DBE	3723	1	0	0	0	0	0	0	3724
		MCE	3236	342	146	0	0	0	0	0	3724
SSI	X	DBE	3724	0	0	0	0	0	0	0	3724
		MCE	3616	108	0	0	0	0	0	0	3724
	Y	DBE	3626	98	0	0	0	0	0	0	3724
		MCE	3137	375	131	81	0	0	0	0	3724

Note: BS: base Shear, Disp: Roof displacement in meters, A–B: details of hinges falling in operational range, B–IO: details of hinges falling in operational and immediate occupancy range, IO–LS: details of hinges falling in immediate occupancy and life safety range, LS–CP: details of hinges falling in life safety and collapse prevention, CP–C: details of hinges falling in collapse prevention and ultimate strength range, C–D: details of hinges falling in ultimate strength and residual strength range, D–E: details of hinges falling in residual strength and failure range.

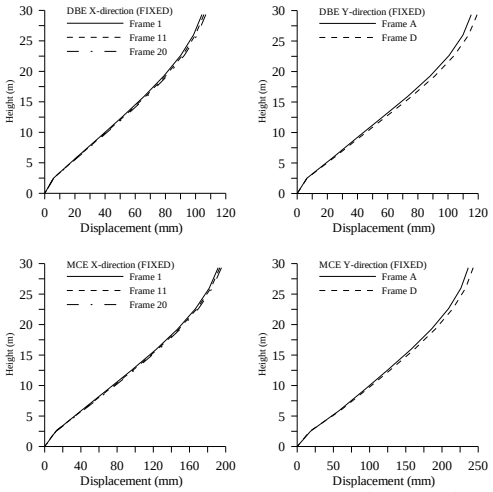

Fig. 17 Displacement along the storey for each frame for fixed base.

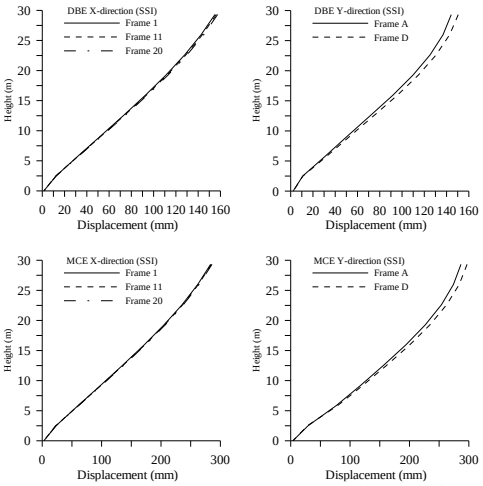

Fig. 18 Displacement along the storey for each frame with SSI.

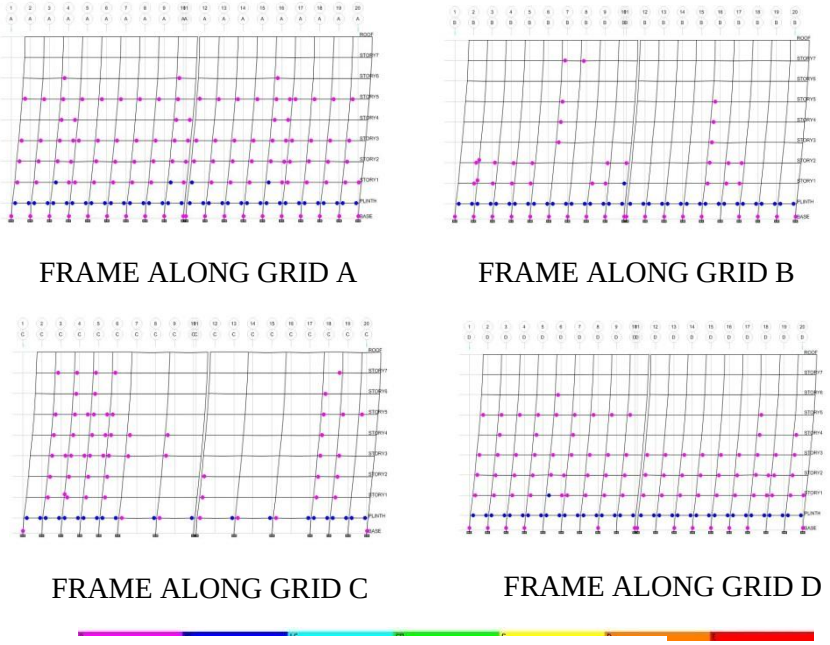

Fig. 15 Plastic hinges at performance point under MCE condition in Y-dir. for fixed.

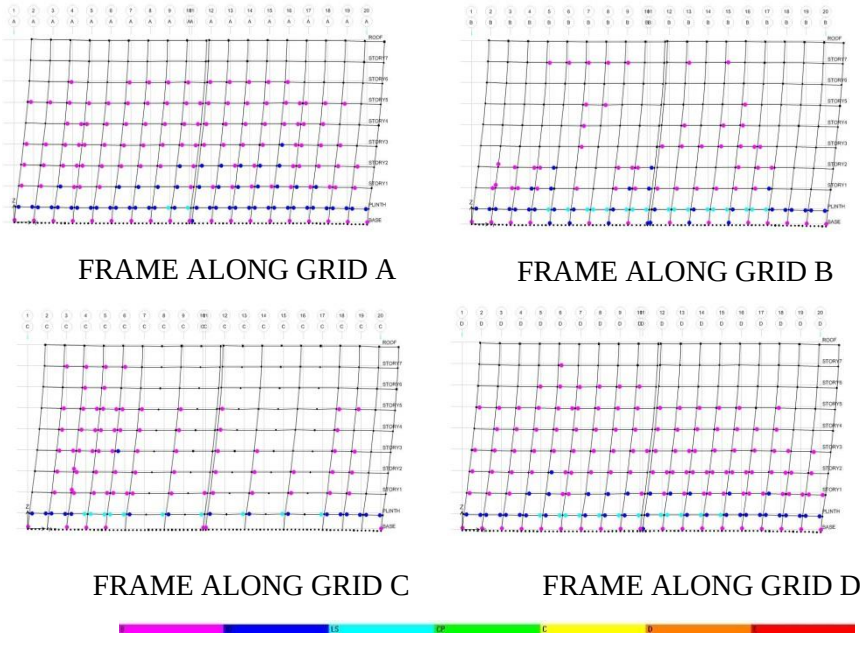

Fig. 16 Plastic hinges at performance point under MCE condition in Y-dir. for SSI.